Optical absorption of semiconducting and metallic nanospheres with the confined electron-phonon coupling

J. D. Lee[a)]
International Center for Young Scientists, National Institute for Materials Science, Tsukuba 305-0044, Japan

(Received 9 December 2005; accepted 30 March 2006; published online 16 May 2006)

We study the optical absorption, especially the (far-) infrared absorption by phonons, of semiconducting and metallic nanospheres. In the nanoscopic sphere, phonons as well as states of electronic excitations are quantized by confinement. It is also known that in the nanoscopic geometry, the confined electron-phonon interaction has a different form from the usual one in the bulk. First, we analyze the phonon and electron contributions to the dielectric response of nanospheres like $\varepsilon(q,\omega)=\varepsilon_{\mathrm{ph}}(q,\omega)+\varepsilon_{\mathrm{el}}(q,\omega)$ or $1/\varepsilon(q,\omega)=1/\varepsilon_{\mathrm{sc-ph}}(q,\omega)+1/\varepsilon_{\mathrm{el}}(q,\omega)$ from the confined electron-phonon interaction for three cases: the intrinsic semiconductor, the doped semiconductor, and the metal. From the dielectric response, the optical absorption spectra are calculated within the semiclassical framework concentrating on the (far-) infrared region and compared to the spectra without imposing confinement. Nontrivial differences of the spectra with confined phonons stem from two features: the electron-phonon coupling matrix has a different form and the phase space q of the confined phonon is reduced because of its quantization to q_n. Finally, size distribution effects in an ensemble of isolated nanospheres are briefly discussed. Those effects are found to be important in metallic spheres with rapid sweepings of resonances by a small change of the sphere size. © *2006 American Institute of Physics*. [DOI: 10.1063/1.2199851]

I. INTRODUCTION

Optical responses of small nanoscopic particles are very different from those of the bulk materials, as a result of the surface effects. For an immediate example, it is well known that silver nanoparticles are yellow and gold nanoparticles red in their states of aqueous sol. These properties have been of vital interest for a long time and extensively studied in recent years.[1,2] It was Mie in 1908 (Ref. 3) who presented a solution to such optical problems of spherical particles by directly solving Maxwell's equations. To date, Mie's classical theory with suitable extensions still deserves attention in promoting renewed theoretical investigation of optical (electromagnetic) characteristics of small particles.

In a system of small size, a particular importance is found in the nonlocal relationship between the electric field $\mathbf{E}$ and the electric displacement $\mathbf{D}$, $\mathbf{D}(\mathbf{r},\omega)=\int d\mathbf{r}'\varepsilon(\mathbf{r},\mathbf{r}';\omega)\mathbf{E}(\mathbf{r}',\omega)$, where $\varepsilon(\mathbf{r},\mathbf{r}';\omega)$ is the nonlocal dielectric function of the sphere.[4] Starting from the above relation, the dynamical polarizability giving the optical absorption has been semiclassically calculated basically following Mie's theory for both semiconductors and metals.[5–8] On the other hand, Eckardt[9] has led the pure quantum mechanical study for the metallic sphere using the local density approximation (LDA) for the self-consistent spherical jellium model, where it is found that excitations of single electron-hole pairs are much stronger and collective modes are slightly redshifted compared to the semiclassical treatments. Nevertheless, the semiclassical Mie theory is still highly valuable and useful because it is the exact solution to Maxwell's equations for the sphere. Recently, with various preparations of samples by advanced fabrication techniques, there evolves a need to understand the role of the surrounding environment in determining the optical properties.[10,11]

Electron-phonon coupling is an important ingredient in determining transport processes, inelastic electron scattering, optical properties, and so on.[12] Many works on optical absorption have been performed in the exciton energy range (for semiconducting spheres) or plasmon energy range (for metallic spheres), while infrared or far-infrared absorption has been relatively unexplored, where phonons would be expected to play a role. It has been reported that the electron-phonon coupling in the nanosphere has a different form from the bulk case because of the quantum confinement arising from a given geometry. For polar materials (such as compound semiconductors), Klein *et al.*[13] and Nomura and Kobayashi[14] have studied how the longitudinal optical (LO) phonons are confined and quantized and derived an expression of the confined electron-LO phonon coupling. They have also examined the size dependence of the Huang-Rhys parameters S, $S=\Sigma_{\mathbf{q}}|\rho_{\mathbf{q}}|^2/\omega_{\mathrm{LO}}$ for the sphere,[15] where $\rho_{\mathbf{q}}$ is the electron-phonon coupling strength and ω_{LO} is the frequency of LO phonon.

In this paper, we study the optical absorption of nanoscopic spheres by accounting for confined phonons. Here, only confined s-wave phonons are considered. It is expected that phonon contributions would result in an appreciable enhancement of the optical absorption in the infrared or far-infrared region for both confined and unconfined phonon cases. However, differences should become important because of two features. One is that the coupling strength of

a)Electronic mail: lee.jaedong@nims.go.jp

confined phonons depends on the sphere radius or other quantities in a different way from that of unconfined phonons. The other is that, for a very small sphere, the phase space allowed for q is strongly suppressed when considering a confinement. Of course, one could expect that as the radius increases both results become identical. In order to incorporate the phonon effect to the optical absorption, we analyze the phonon contribution to the dielectric response $\varepsilon_{\mathrm{ph}}(q,\omega)$ from the confined electron-phonon interaction and then find the total dielectric response of the sphere $\varepsilon(q,\omega)$. Dielectric response makes it possible to evaluate the dynamical polarizability rather straightforwardly within the semiclassical approach.[5–8] We adopt the semiclassical formalism developed by Fuchs and co-workers,[7] merit of which is its wide applicability to any kinds of materials if only the dielectric responses of the corresponding materials are known. Thus we apply the formalism to three kinds of materials: an intrinsic (undoped) semiconductor, a doped semiconductor, and a metal.

The present article is organized as follows. First we start from the Fröhlich Hamiltonian for a bulk polar material and then discuss the confined electron-phonon interaction for the three different cases of an intrinsic (undoped) semiconductor, a doped semiconductor, and a metal in Sec. II. In the section, phonon contributions to the dielectric response $\varepsilon_{\mathrm{ph}}(q,\omega)$ are obtained for each different material. In Sec. III, we evaluate the optical absorption of nanosphere with respect to its radius from the far-infrared region ($\ll\omega_{\mathrm{LO}}$) to $\sim\omega_{\mathrm{pl}}$ (plasmon frequency for a metal or a doped semiconductor) or $\sim\omega_{\mathrm{ex}}$ (exciton frequency for an undoped semiconductor). The results are compared to cases with unconfined phonons. We also briefly discuss the effects of the size distribution in the optical absorption of a collection of metallic spheres. Finally, in Sec. IV, we give concluding remarks.

II. CONFINED PHONON COUPLING AND DIELECTRIC RESPONSE $\varepsilon_{\mathrm{ph}}(q,\omega)$

The coupling between electron and LO phonon can be very large in a polar solid such as an ionic crystal or semiconductor, where the polarization set up by exciting LO phonons causes an electric field which scatters electron. In this section, beginning with a brief explanation of the Fröhlich Hamiltonian for a bulk polar material, we derive the electron-phonon coupling and analyze its contribution to the dielectric response $\varepsilon_{\mathrm{ph}}(q,\omega)$ for several different cases of nanospheres. Here it is worth discussing the validity of the form of $\varepsilon_{\mathrm{ph}}(q,\omega)$ for the nanosystem. The nonlocal dielectric function $\varepsilon(q,\omega)$ from the Fourier transform of $\varepsilon(\mathbf{r}-\mathbf{r}',\omega)$ is a consequence of the isotropy of the medium. It is clear that such an isotropy is broken by a surface or an interface of the nanosystem. Nevertheless, our treatment may be justified by the recent reports by Delerue *et al.*[16] and Giustino and Pasquarello.[17] Delerue *et al.* have demonstrated that the static bulk screening can be effective at distances of the order of just a few Fermi wavelengths from the boundary through investigating the screened field in Si layers. In addition, Giustino and Pasquarello have reported that, in similar Si slabs, the high-frequency permittivity closely matches the bulk value beyond 13 Si monolayers (about 18 Å).

A. Fröhlich Hamiltonian

It is well known that the interaction between electrons and bulk LO phonons, the so-called Fröhlich Hamiltonian, is written as[18]

$$\mathcal{H}=\sum_{\mathbf{q}}\frac{\sqrt{2\pi\omega_{\mathrm{LO}}}}{\nu^{1/2}q}\left[\frac{1}{\varepsilon_{\infty}}-\frac{1}{\varepsilon_{0}}\right]^{1/2}\sum_{\mathbf{k}}c_{\mathbf{k}}^{\dagger}c_{\mathbf{k}+\mathbf{q}}(a_{-\mathbf{q}}+a_{\mathbf{q}}^{\dagger}),\qquad(1)$$

where $c_{\mathbf{k}}^{\dagger}(c_{\mathbf{k}+\mathbf{q}})$ and $a_{\mathbf{q}}^{\dagger}(a_{-\mathbf{q}})$ are the electron creation (annihilation) and phonon creation (annihilation) operators, respectively. ε_0 is the low-frequency dielectric constant, ε_∞ is from the interband electronic transitions, and ω_{LO} is the frequency of the LO phonon. ν is the volume of the system. $\mathcal{H}$ can be expected to be most suitably applied to the conduction bands of a (bulk) semiconductor. Now we can find the dielectric function by investigating the effective interaction between electrons,

$$V_{\mathrm{eff}}(q,\omega)=\frac{4\pi/q^{2}}{\varepsilon(q,\omega)}=\frac{v_{q}}{\varepsilon(q,\omega)},\qquad(2)$$

where $\varepsilon(q,\omega)$ corresponds to the total dielectric response. Diagrams of electron-electron scattering and electron-phonon scattering can be summed by writing down the combined interaction $W(q,\omega)$ of the Coulomb interaction and the electron-phonon interaction as

$$W(q,\omega)=v_{q}/\varepsilon_{\infty}+V_{\mathrm{ph}}(q,\omega),\qquad(3)$$

and the screened effective interaction $V_{\mathrm{eff}}(q,\omega)$ becomes

$$V_{\mathrm{eff}}(q,\omega)=\frac{W(q,\omega)}{1-W(q,\omega)P(q,\omega)},\qquad(4)$$

where $P(q,\omega)$ is the polarization function of electrons. Putting the total dielectric response as a sum of the phonon and electron contributions, i.e.,

$$\varepsilon(q,\omega)=\varepsilon_{\mathrm{ph}}(q,\omega)+\varepsilon_{\mathrm{el}}(q,\omega),\qquad(5)$$

one can find

$$\varepsilon_{\mathrm{ph}}(q,\omega)=v_{q}/W(q,\omega).\qquad(6)$$

The next step is to find $W(q,\omega)$ from the specific Hamiltonian $\mathcal{H}$. It is clear that $V_{\mathrm{ph}}(q,\omega)$ out of $W(q,\omega)$ can be interpreted as the product $|M_q|^2\mathcal{D}_0(q,\omega)$, where M_q is the electron-phonon scattering vertex,

$$M_{q}=\frac{\sqrt{2\pi\omega_{\mathrm{LO}}}}{q}\left[\frac{1}{\varepsilon_{\infty}}-\frac{1}{\varepsilon_{0}}\right]^{1/2},$$

and $\mathcal{D}_0(q,\omega)$ is Green's function of the corresponding phonon, i.e.,

$$\mathcal{D}_{0}(q,\omega)=\frac{2\omega_{\mathrm{LO}}}{\omega^{2}-\omega_{\mathrm{LO}}^{2}}$$

in the present case. Then $V_{\mathrm{ph}}(q,\omega)$ becomes

$$V_{\mathrm{ph}}(q,\omega)=v_q\frac{\omega_{\mathrm{LO}}^2}{\omega^2-\omega_{\mathrm{LO}}^2}\left[\frac{1}{\varepsilon_\infty}-\frac{1}{\varepsilon_0}\right]. \tag{7}$$

By substituting Eq. (7) into Eq. (6), we finally find a well-known $\varepsilon_{\mathrm{ph}}(q,\omega)$ for polar materials,[18]

$$\varepsilon_{\mathrm{ph}}(q,\omega)=\varepsilon_\infty\frac{\omega^2-\omega_{\mathrm{LO}}^2}{\omega^2-\omega_{\mathrm{TO}}^2}, \tag{8}$$

where ω_{TO} is the frequency of the transverse optical (TO) phonon. Note that in deriving Eq. (8), we have used the Lyddane-Sachs-Teller (LST) relation of

$$\frac{\omega_{\mathrm{LO}}^2}{\omega_{\mathrm{TO}}^2}=\frac{\varepsilon_0}{\varepsilon_\infty}.$$

B. Nanosphere of an intrinsic (undoped) semiconductor

Exciton states play an important role in the understanding of interband transitions in intrinsic semiconductors. Klein *et al.*[13] and Nomura and Kobayashi[14] have investigated the exciton-LO phonon coupling in semiconductor microcrystallites with phonon confinement effects included. Starting with the Fröhlich Hamiltonian, they found the electric potential $\phi(\mathbf{r})$ induced by spherical LO phonons $a_{lm}(q)$ [or $a_{lm}(q)^\dagger$] to be

$$\phi(\mathbf{r})=\sum_{lm}\sum_q f_l(q)[a_{lm}(q)j_l(qr)Y_{lm}(\theta,\varphi)+\mathrm{H.c.}] \tag{9}$$

and have incorporated additional boundary conditions, one of which is for a freestanding sphere. It corresponds to the condition $\nabla\cdot\mathbf{u}=0$ at the surface, where $\mathbf{u}$ is the displacement, and leads to a vanishing potential $\phi=0$ at the surface,

$$j_l(qR)=0,$$

where $j_l(x)$ is the spherical Bessel function of order l and R is the radius of the sphere, in terms of which q is quantized as q_{ln}. $f_l(q)$ is also slightly changed from the Fröhlich Hamiltonian into

$$f_l(q)=B_q\frac{\sqrt{2\pi\omega_{\mathrm{LO}}}}{\nu^{1/2}q}\left[\frac{1}{\varepsilon_\infty}-\frac{1}{\varepsilon_0}\right]^{1/2}, \tag{10}$$

where B_q is the normalization constant satisfying $B_qB_{q'}\int d\mathbf{r}j_l(qr)Y_{lm}^*(\theta,\varphi)j_{l'}(q'r)Y_{l'm'}(\theta,\varphi)=\delta_{qq'}\delta_{ll'}\delta_{mm'}$, that is, $B_q^2=2/[R^3j_{l+1}^2(qR)]$. For the s-wave phonon, we have simply $B_q=\sqrt{2}q/R^{1/2}$. Hereafter we treat only the s-wave ($l=0$) phonon, unless specified otherwise. q_{ln} can then be assigned as $q_n=n\pi/R$. ν is a volume of the sphere. Now we can write down the exciton-LO phonon interaction Hamiltonian by assuming the charge density $\rho_{\mathrm{ex}}^c(\mathbf{r})$ for a Wannier exciton confined inside the sphere, from Eqs. (9) and (10),

$$\mathcal{H}=\int d\mathbf{r}\ \phi(\mathbf{r})\rho_{\mathrm{ex}}^c(\mathbf{r}).$$

As shown above, for the exciton-LO phonon coupling, it is of importance to precisely determine the wave functions of an electron and a hole. In fact, this topic has already been widely investigated.[19] Performing an explicit integration for $\mathcal{H}$, we find

$$\mathcal{H}=\sum_n\frac{\sqrt{2\pi\omega_{\mathrm{LO}}}}{\nu^{1/2}q_n}\left[\frac{1}{\varepsilon_\infty}-\frac{1}{\varepsilon_0}\right]^{1/2}\times\sum_{\lambda\mu}\rho_{\lambda\mu}(q_n)\psi_\lambda^\dagger\psi_\mu[a(q_n)+a(q_n)^\dagger], \tag{11}$$

where $\psi_\lambda^\dagger(\psi_\mu)$ denotes the operator for creating (annihilating) an exciton with the quantum number $\lambda(\mu)$ and the scattering matrix $\rho(q)$ is, keeping only $\lambda=\mu=1s$ exciton states and considering the simplest hydrogenic states,

$$\rho_{\mathrm{ex}}^c(\mathbf{r})=\frac{1}{\pi(\eta_ha_0)^3}e^{-2r/\eta_ha_0}-\frac{1}{\pi(\eta_ea_0)^3}e^{-2r/\eta_ea_0},$$
$$\rho(q)\approx\sqrt{\frac{2}{3}}qR\left[\frac{1}{(1+q^2\eta_h^2a_0^2/4)^2}+\frac{1}{(1+q^2\eta_e^2a_0^2/4)^2}\right], \tag{12}$$

where η_e and η_h are defined as $m_h^*/(m_e^*+m_h^*)$ and $m_e^*/(m_e^*+m_h^*)$, respectively. m_e^* and m_h^* are the effective masses of the electron and the hole, respectively. We define $a_{\mathrm{ex}}\equiv\eta_ea_0$, where $a_0=(\epsilon/\mu)a_B$ ($a_B=0.53$ Å, i.e., Bohr radius) for Coulomb attraction $-1/\epsilon|\mathbf{r}|$ between electron and hole and μ is a reduced mass, $\mu=m_e^*m_h^*/(m_e^*+m_h^*)$. The electric potential induced by LO phonon is given by the difference between contributions of electron ($\mathbf{r}_e=\eta_e\mathbf{r}$; $\mathbf{r}=\mathbf{r}_e-\mathbf{r}_h$) and hole ($\mathbf{r}_h=-\eta_h\mathbf{r}$), from which we can express $\rho_{\mathrm{ex}}^c(\mathbf{r})$ as the difference between electron's and hole's[14,19] like $\int d\mathbf{r}[\phi(\eta_hr)-\phi(\eta_er)]|\psi(r)|^2=\int d\mathbf{r}\ \phi(r)\rho_{\mathrm{ex}}^c(r)$, where $|\psi(r)|^2=e^{-2r/a_0}/(\pi a_0^3)$ for $1s$ exciton state.[20] Furthermore it is based on the hydrogenic wave function of an exciton, that is, an exciton is so weakly confined in a sphere that the envelop function of an exciton is kept as in the bulk. Hence our model will be hereafter applied to $R>a_{\mathrm{ex}}$. For a plane-wave phonon interacting with the same exciton, we obtain the slightly different matrix

$$\rho(q)\approx\frac{1}{(1+q^2\eta_h^2a_0^2/4)^2}-\frac{1}{(1+q^2\eta_e^2a_0^2/4)^2}. \tag{13}$$

Although Eqs. (12) and (13) show similar matrix behaviors, one may note an important conceptual difference. Let us think of the limit of reducing the radius R with $a_{\mathrm{ex}}=R$ fixed. Reducing the sphere size leads to an increasing overlap of the electron and hole wave functions (i.e., $a_{\mathrm{ex}}\to0$) and finally makes $\rho(q)\to0$, in the case of unconfined coupling.[21] On the contrary, however, in the case of the confined coupling, the same reduction in size should lead to an increasing coupling of short wavelength phonons ($q\sim1/a_{\mathrm{ex}}$), which compensates an increasing overlap of the electron and hole wave functions.

Now we analyze the phonon contribution to the dielectric response exploiting Eq. (6);

$$\varepsilon_{\mathrm{ph}}(q,\omega)=\frac{\varepsilon_\infty(\omega^2-\omega_{\mathrm{LO}}^2)}{(\omega^2-\omega_{\mathrm{LO}}^2)+|\rho(q)|^2(\omega_{\mathrm{LO}}^2-\omega_{\mathrm{TO}}^2)}, \tag{14}$$

where in a case of the confined model, Eq. (12) should be used for $\rho(q)$, while in a case of the unconfined model, Eq.

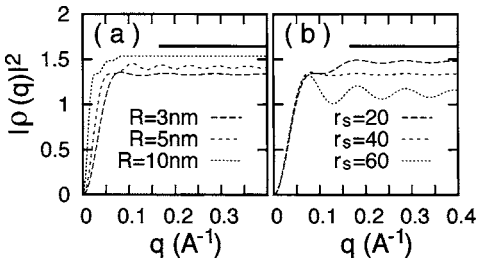

FIG. 1. Behavior of $|\rho(q)|^2$ for a doped semiconductor nanosphere with respect to (a) the radius (R) of the sphere for a fixed $r_s=40$ and (b) the electron density (r_s) for a fixed $R=3$ nm. Here r_s is the electron density parameter defined by $4\pi r_s^3/3=1/n$ (n: electron density), that is, $r_s=20$, $r_s=40$, and $r_s=60$ correspond to the electron densities of $n\sim 2\times 10^{20}$, $\sim 2.5\times 10^{19}$, and $\sim 7.4\times 10^{18}$ cm^{-3}, respectively. The calculation is done by taking an angular average for $k=k_F$ (k_F: Fermi wave vector) in Eq. (17). The thick solid line is the value of $\pi^2/6$ for $R\to\infty$.

(13) should be used for $\rho(q)$. Later, for a calculation of the optical contributions of $\varepsilon_{\mathrm{ph}}(q,\omega)$, ω^2 in Eq. (14) may be replaced by $\omega(\omega+i\gamma_{\mathrm{ph}})$. On the other hand, we will adopt the dielectric response of the electronic part (the exciton dielectric function in the present case) from the hydrodynamic model,[7,10]

$$\varepsilon_{\mathrm{ex}}(q,\omega)=\frac{f_p^2}{\omega_{\mathrm{ex}}^2+Dq^2-\omega(\omega+i\gamma)}, \tag{15}$$

where f_p is the oscillator strength, ω_{ex} is the exciton energy, $D=\omega_{\mathrm{ex}}/M$ (M: the exciton mass), and γ is the damping constant. The total dielectric response is then $\varepsilon(q,\omega)=\varepsilon_{\mathrm{ph}}(q,\omega)+\varepsilon_{\mathrm{ex}}(q,\omega)$.

C. Nanosphere of a doped semiconductor

We deal with a semiconductor which is doped enough to give a degenerate electron gas. The intraband transition in such a heavily doped semiconductor is usually treated like a metal. Following the same route as for the sphere of an intrinsic semiconductor, $\mathcal{H}$ can be readily written as

$$\mathcal{H}=\sum_n \frac{\sqrt{2\pi\omega_{\mathrm{LO}}}}{\nu^{1/2}q_n}\left[\frac{1}{\varepsilon_\infty}-\frac{1}{\varepsilon_0}\right]^{1/2} \times\sum_{\lambda\mu}\rho_{\lambda\mu}(q_n)c_\lambda^\dagger c_\mu[a(q_n)+a(q_n)^\dagger], \tag{16}$$

where $c_\lambda^\dagger(c_\mu)$ is now the electron operator as in Eq. (1). Considering that conduction electrons are also confined inside the sphere, the scattering matrix $\rho(q)$ should be, originally,

$$\rho(q;k,k')=\frac{\nu^{1/2}}{\sqrt{4\pi}}B_qB_kB_{k'}\int_0^R dr\, r^2 j_0(qr)j_0(kr)j_0(k'r). \tag{17}$$

For $R\to\infty$ in Eq. (17), an integration of $\rho(q;k,k')$ gives $\pi/\sqrt{6}$ only when $k'=|\mathbf{k}+\mathbf{q}|$, otherwise it vanishes. For a finite R, $\rho(q;k,k')$ is evaluated by keeping $k=k_F$ and taking an average over an angle between $\mathbf{k}$ and $\mathbf{q}$ of $k'=|\mathbf{k}+\mathbf{q}|$, with which $\rho(q;k,k')$ is reduced to $\rho(q)$. Figure 1 shows the numerical integration of $\rho(q)$. The integral depends on the doped electron density. The more electrons, the faster $|\rho(q)|^2$ approaches $\pi^2/6$. Incidentally, values of $|\rho(q)|^2$ in the $l=1$ channel are smaller by at least an order of magnitude. Of course, in the unconfined model, $|\rho(q)|^2$ should be 1. By the way, a similar definition is found for the Huang-Rhys parameter[15] S, which also characterizes a strength of electron-phonon coupling. An essential difference is that S estimates an interaction energy of phonon with the ground state electron density, $S\propto(1/\omega_{\mathrm{LO}})\Sigma_q B_q^2|\int_0^R dr\, r^2 j_0(qr)\times[j_0(\pi r/R)]^2|^2$, but $|\rho(q)|^2$ in Eq. (17) estimates a coupling strength of phonon with the electron density near the Fermi surface. Due to such a difference, $|\rho(q)|^2$ increases with R and approaches a limiting value, but S decreases with R and approaches a limiting value with small additional structures.[22]

The phonon contribution $\varepsilon_{\mathrm{ph}}(q,\omega)$ is formally identical to Eq. (14) for an intrinsic semiconductor except that $|\rho(q)|^2$ of Eq. (17) should be used. Taking the electronic contribution $\varepsilon_{\mathrm{el}}(q,\omega)$ from the hydrodynamic model,[7,10] we finally have

$$\varepsilon(q,\omega)=\frac{\varepsilon_\infty(\omega^2-\omega_{\mathrm{LO}}^2)}{(\omega^2-\omega_{\mathrm{LO}}^2)+|\rho(q)|^2(\omega_{\mathrm{LO}}^2-\omega_{\mathrm{TO}}^2)} -\frac{\omega_{\mathrm{pl}}^2}{\omega(\omega+i\gamma)-\beta^2q^2}, \tag{18}$$

where ω_{pl} is the plasmon energy, γ is the damping constant, and $\beta^2=(3/5)v_F^2$ (v_F: the Fermi velocity).

D. Nanosphere of a metal

For a metallic nanosphere, the situation is rather similar to the doped semiconductor. One can arrive at the metallic electron-phonon interaction by replacing ω_{LO} with ω_{ip}, where ω_{ip} is the ion plasma frequency, and also by setting $[1/\varepsilon_\infty-1/\varepsilon_0]^{1/2}$ to 1. In other words, we now have $\omega_{\mathrm{TO}}=0$ in the metal. The ion plasma frequency ω_{ip} is related to the plasmon frequency ω_{pl} by

$$\omega_{\mathrm{ip}}^2=\frac{Zm}{M}\omega_{\mathrm{pl}}^2.$$

Z is the valence of the ion and m and M are the electron and ion masses, respectively. The long wavelength excitation of the coupled system of ions and conduction (free) electrons is the acoustic phonon, which is also readily understood from the polar coupling on an equal footing with the doped semiconductor: $\omega^2=\omega_{\mathrm{TO}}^2+(\omega_{\mathrm{LO}}^2-\omega_{\mathrm{TO}}^2)/\varepsilon(q)$. Accounting for the electron screening by realizing the static dielectric function $\varepsilon(q)\to\omega_{\mathrm{pl}}^2/\beta^2q^2$ [using $\varepsilon_{\mathrm{el}}(q,\omega)$ out of Eq. (18); $\beta^2=\frac{3}{5}v_F^2$], we have in the metallic case $\lim_{q\to 0}\omega(q)=\sqrt{\omega_{\mathrm{ip}}/\omega_{\mathrm{pl}}}\beta q$. Now, for the metallic nanosphere with confined excitations, we write $\mathcal{H}$ as follows:

$$\mathcal{H}=\sum_n\frac{\sqrt{2\pi\omega_{\mathrm{ip}}}}{\nu^{1/2}q_n}\sum_{\lambda\mu}\rho_{\lambda\mu}(q_n)c_\lambda^\dagger c_\mu[a(q_n)+a(q_n)^\dagger]. \tag{19}$$

The scattering matrix $\rho(q)$ is defined in the same way as that of the doped semiconductor. But in the metallic case, for example, we have $r_s=2.07$ for Al, which is an extremely high density compared to the case of the doped semiconductor. In this case, we can have practically $\rho(q)=\pi/\sqrt{6}$ unlike the doped semiconductor.

In the metallic case, the typical energy scale of ω_{pl} is much larger than ω_{ip}. In this case, it is conventional (although not necessarily required) to separate the electron-electron part and the electron-phonon part like

$$\frac{1}{\varepsilon(q,\omega)} = \frac{1}{\varepsilon_{sc-ph}(q,\omega)} + \frac{1}{\varepsilon_{el}(q,\omega)}$$

rather than $\varepsilon(q,\omega)=\varepsilon_{ph}(q,\omega)+\varepsilon_{el}(q,\omega)$. Here we note that $\varepsilon_{el}(q,\omega)$ is

$$\varepsilon_{el}(q,\omega) = 1 - \frac{\omega_{pl}^2}{\omega(\omega+i\gamma)-\beta^2 q^2}.$$

In the present case, $\varepsilon_{sc-ph}(q,\omega)$ describes the screened electron-phonon interaction. By the argument given in Sec. II A, one may find

$$\frac{1}{\varepsilon_{sc-ph}(q,\omega)} = \frac{1}{v_q}\frac{M_q^2|\rho(q)|^2}{\varepsilon_{el}(q,\omega)^2}\mathcal{D}(q,\omega), \tag{20}$$

where M_q is $\sqrt{2\pi\omega_{ip}}/q$. In Eq. (20), $\mathcal{D}(q,\omega)$ is the interacting phonon Green's function,

$$\mathcal{D}(q,\omega) = \frac{2\omega_{ip}}{[\omega^2-\omega_{ip}^2-2\omega_{ip}M_q^2|\rho(q)|^2P(q,\omega)/\varepsilon_{el}(q,\omega)]}, \tag{21}$$

and $P(q,\omega)$ is the electron polarization function, $P(q,\omega)=[1-\varepsilon_{el}(q,\omega)]/v_q$. Because of the apparent separation of energy scales of electron and phonon, one may simplify the expression by putting $\omega=0$ in $P(q,\omega)$ and $\varepsilon_{el}(q,\omega)$ in Eq. (21).

E. Quantization in dielectric responses

The quantization of phonons by confinement has been described in detail in former sections, through which the matrix elements by the confined electron-phonon coupling have been calculated. We also consider that electronic excitations are quantized for the confined model. Cini and Ascarelli[23] have obtained an extended RPA (i.e., random phase approximation) expression starting from confined single electron wave functions with $k_m=m\pi/L$ in a cubic box of side L, which is given as a summation of approximate delta functions centered at $q=q_n$ ($q_n=n\pi/L$). A general treatment of the spherical model is complicated and cumbersome. The electronic susceptibility $\chi(q,\omega)$ out of $\varepsilon(q,\omega)^{-1}=1+v(q)\chi(q,\omega)$ includes contributions of all orders l.[24] Collective excitations would be subject to the spherical wave quantization. For the low energy branch of excitations, we can assume the s-wave quantization because $q_n=n\pi/R$ for the s wave allows smaller value of q_n (i.e., smaller excitation energy) for a given n than any other order spherical wave. It should be noted that Cini and Ascarelli's cubic box model has been introduced to avoid difficulties in a treatment of a spherical model. Wood and Aschcroft[6] have further developed the cubic model by arguing that energy and general behavior of a cube and a sphere will differ only by geometric factors of the order of 1. This signifies that the detailed quantization condition depending on the geometry is not so crucial that the dielectric responses of a spherical particle have a similar quantized structure with those of a cubic particle.

Following Cini and Ascarelli,[23] we propose that, within the spherical quantization, the spectral function of the system, i.e., $\propto -\mathrm{Im}[1/\varepsilon_{confined}(q,\omega)]$, be written as

$$-\mathrm{Im}\left[\frac{1}{\varepsilon_{confined}(q,\omega)}\right] \approx -\frac{\pi}{R}\sum_{q_n}\mathrm{Im}\left[\frac{1}{\varepsilon(q,\omega)}\right]\delta(q-q_n),$$

which may be directly measured by electron energy loss spectroscopy (EELS). It should be given as a sum of contributions from discrete modes of q_n by the spherical quantization. By the Kramers-Kronig relation, the real part of $1/\varepsilon_{confined}(q,\omega)$ is

$$\mathrm{Re}\left[\frac{1}{\varepsilon_{confined}(q,\omega)}\right] = 1 - \frac{\pi}{R}\sum_{q_n}\delta(q-q_n) + \frac{\pi}{R}\sum_{q_n}\mathrm{Re}\left[\frac{1}{\varepsilon(q,\omega)}\right]\delta(q-q_n).$$

The above expressions for $\mathrm{Re}[1/\varepsilon_{confined}(q,\omega)]$ and $\mathrm{Im}[1/\varepsilon_{confined}(q,\omega)]$ trivially give $1/\varepsilon_{confined}(q,\omega)=1$ for $q\neq q_n$. Accordingly, $1/\varepsilon_{confined}(q,\omega)$ can be written down as

$$\frac{1}{\varepsilon_{confined}(q,\omega)} \approx \frac{\pi}{R}\sum_{q_n}\left[\frac{1}{\varepsilon(q,\omega)}-1\right]\delta(q-q_n)+1, \tag{22}$$

where $\varepsilon(q,\omega)=\varepsilon_{ph}(q,\omega)+\varepsilon_{el}(q,\omega)$, or $1/[\varepsilon(q_n,\omega)]=1/\varepsilon_{sc-ph}(q,\omega)+1/\varepsilon_{el}(q,\omega)$ with the confined electron-phonon coupling, as obtained in the previous sections. It is worth noting that $1/\varepsilon_{confined}(q,\omega)$ self-evidently satisfies the Kramers-Kronig relation, which implies that the related sum rule such as f-sum rule can be obeyed.[18]

III. OPTICAL ABSORPTION

A. Response of a single sphere

We consider a single sphere of radius R. Its response to the arbitrary electric field is characterized by polarizabilities α_l, where l is the pole order of the external electric field. By solving Maxwell's equations for an isolated sphere in vacuum with the usual boundary conditions,[25] i.e., $\nabla\cdot\mathbf{D}=0$ and $\nabla\times\mathbf{E}=0$, Fuchs and co-workers[7] developed a semiclassical theory and obtained the result for the polarizability of order l,

$$\alpha_l(\omega) = \frac{l(E_l-1)}{l(E_l+1)+1}R^{2l+1}, \tag{23}$$

where, accounting for the nonlocal dielectric response, E_l is given by

$$E_l^{-1} = \frac{2}{\pi}(2l+1)R\int_0^\infty dq\frac{[j_l(qR)]^2}{\varepsilon(q,\omega)}. \tag{24}$$

If we neglect the nonlocality in Eq. (23), i.e., $\varepsilon(q,\omega)=\varepsilon(\omega)$, we obtain the polarizability from a simple substitution of $E_l=\varepsilon(\omega)$ in Eq. (23). Finally, the optical absorption is obtained by taking the imaginary part of the polarizability, i.e., $-\mathrm{Im}[\alpha_l(\omega)]$. In the following sections, Eq. (24) is applied for the calculation of the absorption in the unconfined model

using the dielectric function with the unconfined electron-phonon coupling and with continuous q's. In Secs. II B–II D, we have provided expressions of the dielectric functions with both unconfined and confined electron-phonon couplings. On the other hand, for a case of the confined model, we explore another formula extended from the semiclassical framework of Fuchs and co-workers[7] with $1/\varepsilon(q,\omega)$ replaced by $1/\varepsilon_{\text{confined}}(q,\omega)$ in Eq. (24). E_l^{-1} is then changed to

$$E_l^{-1} = 2(2l+1)\sum_n [j_l(q_nR)]^2 \frac{1}{\varepsilon(q_n,\omega)}, \tag{25}$$

where we have exploited a trial relation of $\Sigma_n[j_l(q_nR)]^2 = \Sigma_n[j_l(n\pi)]^2 = 1/[2(2l+1)]$.[26] In Eq. (25), $\varepsilon(q_n,\omega)$ should be one with the confined electron-phonon coupling. One may find a continuous approach of Eq. (25) to Eq. (24) with increasing sphere radius R.

If we assume a uniform electric field $\mathbf{E}=E(\omega)\hat{z}$, only the dipolar component ($l=1$) survives. For $l=1$, the polarizability α_1 is proportional to R^3. In this study, we always consider only the dipole absorption and give the optical absorption as $-\text{Im}[\alpha_1(\omega)]/R^3$ unless otherwise mentioned. By the way, it is, in principle, straightforward to go to higher polar absorption.

B. Nanosphere of an intrinsic (undoped) semiconductor

We investigate the optical absorption including the infrared region for a ZnSe sphere. The total dielectric response of the sphere should be given as a sum of $\varepsilon_{\text{ph}}(q,\omega)$ and $\varepsilon_{\text{ex}}(q,\omega)$ from Eqs. (14) and (15). But in $\varepsilon_{\text{ph}}(q,\omega)$ we replace ω^2 by $\omega(\omega+i\gamma_{\text{ph}})$. Corresponding to a ZnSe nanosphere, we employ values for various parameters: $f_p/\omega_{\text{ex}}=0.074$, $D/c^2=6.173\times10^{-6}$ (c is the speed of light), $\gamma_{\text{ex}}/\omega_{\text{ex}}=0.01$ and $\omega_{\text{ex}}=2.8$ eV from Ref. 27; and $\omega_{\text{LO}}=30.5$ meV, $\omega_{\text{TO}}=25.7$ meV, $\varepsilon_\infty=5.9$, $m_e^*=0.171$, $m_h^*=0.60$, and $\gamma_{\text{ph}}/\omega_{\text{ex}}=10^{-5}$ from Ref. 28. The evaluated value of a_{ex} for ZnSe is $a_{\text{ex}}\approx 2.6$ nm. But in the study, we regard a_{ex} as a free parameter (adopting the others from ZnSe parameters) and examine the absorption behavior with respect to R and a_{ex}.

Figure 2 shows the absorption of a ZnSe sphere confining a single exciton in the infrared region. Peaks in the absorption spectra are determined by $\text{Re}[E_1(\omega)]+2=0$ from Eqs. (22) and (25), not by $\text{Re}[E_1(\omega)]=0$. Resonances by $\text{Re}[E_1(\omega)]+2=0$ should be noticed to be the excitations arising from the presence of the surface. A single resonance peak is dominant in the infrared absorption spectra for a ZnSe sphere and its position depends on R and a_{ex} through the electron-phonon matrix $|\tilde{\rho}(q)|^2$. We further note that $\text{Re}[E_1(\omega)]+2=0$ can be readily satisfied near $\text{Re}[E_1(\omega)]\to-\infty$, i.e., $\text{Re}[E_1^{-1}(\omega)]=0$. Unless the sphere is too small, we can write down an equation determining the surface resonance,

$$\frac{1}{6}(\omega^2-\omega_{\text{LO}}^2)+(\omega_{\text{LO}}^2-\omega_{\text{TO}}^2)\sum_n |\tilde{\rho}(q_n)|^2[j_l(q_nR)]^2 \approx 0.$$

In this equation, the second term is positive definite and thus the zero should always be found to be less than ω_{LO}. One can

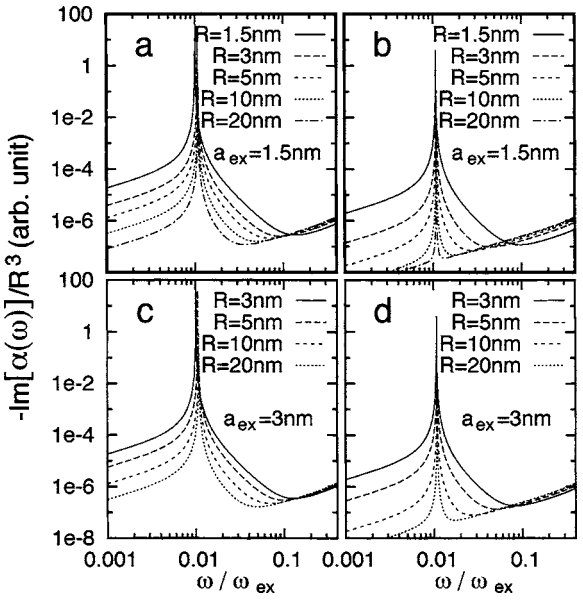

FIG. 2. Absorption of a ZnSe sphere in the (far-) infrared region for various R's and $a_{\text{ex}}=1.5$ nm and $a_{\text{ex}}=3$ nm. (a) and (c) are for confined electron-phonon coupling, while (b) and (d) are for unconfined (plane-wave) electron-phonon coupling.

check from Fig. 2 that the resonance peaks are always less than 0.011 ($=\omega_{\text{LO}}/\omega_{\text{ex}}$). In the figure, we compare the optical absorption of the sphere with confined and unconfined electron-phonon couplings for various R's with a fixed a_{ex}. Two noticeable differences are found. One is the redshift of phonon peaks in the confined model, where the redshift is strengthened as R gets smaller. The other is the absorption strength. The absorption with confined phonons is found to be stronger than that with unconfined phonons by about two orders of magnitude. Besides, it may also be worth noticing that the phonon absorption for $R=a_{\text{ex}}=1.5$ nm in Fig. 2(a) and that for $R=a_{\text{ex}}=3$ nm in Fig. 2(c) are almost identical. The same is also found in Figs. 2(b) and 2(d). We realize that $|\tilde{\rho}(q_n)|^2$ should be simplified for $R=a_{\text{ex}}$ as

$$|\tilde{\rho}(q_n)|^2 = \frac{2}{3}(n\pi)^2\left[\frac{1}{(1+0.285^2n^2\pi^2/4)^2} - \frac{1}{(1+n^2\pi^2/4)^2}\right]^2$$
$$\approx \frac{2}{3}\frac{16^2}{(n\pi)^6}\left[\frac{1}{0.285^4}-1\right]^2 \quad \text{when } n \gg 1,$$

where n should be 1,2,3,… and 0.285 is m_e^*/m_h^*. That is, in $|\tilde{\rho}(q_n)|^2$ when $R=a_{\text{ex}}$, one cannot find any dependence on R (or a_{ex}). It is natural that the absorption is vanishingly small in the limit of $R\gg a_{\text{ex}}$. By the way, Chamberlain *et al.*[29] have studied the Raman scattering of CdS nanosphere in the infrared region using a continuum model of vibration and electrostatic potential. The difference of their model from ours is that they have taken into account the coupling between longitudinal and transverse modes. They have obtained the overwhelming lowest order phonon peak consistent with the peak in Fig. 2 and minute higher order structures disappearing when $R\gtrsim 2$ nm. The main phonon peak is larger than higher order structures by several orders of magnitudes and is al-

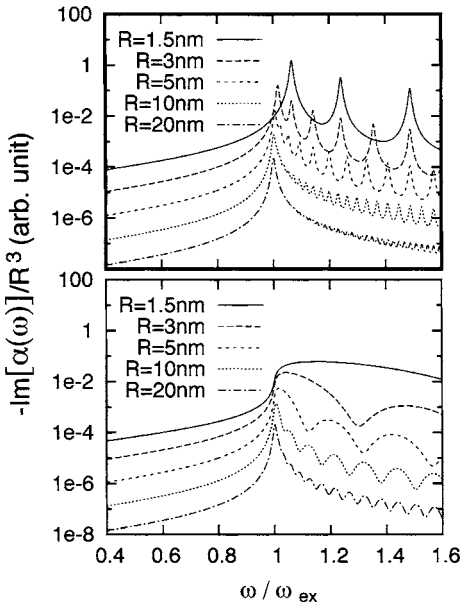

FIG. 3. Absorption of a ZnSe sphere in the exciton energy region. The upper panel gives the absorption for the confined model and the lower panel for the unconfined model. Here a_{ex} is fixed as $a_{ex}=1.5$ nm. Note that for a better presentation, data of $R=1.5$ nm, $R=3$ nm, $R=10$ nm, and $R=20$ nm are shifted by multiplying by 100, 10, 0.1, and 0.01, respectively.

most exclusively due to the $l=0$ electron and hole contributions arising from interaction with the $l=0$ phonons, which is corresponding to our case.

Figure 3 shows the absorption spectra of a ZnSe sphere in the exciton energy range, $\omega \sim \omega_{ex}$. First, we confirm that the frequency of the exciton peak increases with decreasing sphere size.[7] A series of small peaks above the exciton peak, the effect of nonlocal dielectric responses, is observed for both confined and unconfined excitations. However, in the case with confined excitations, we have more sharply defined resonances. For a sphere with a large enough radius, we can get the same spectra for both types of excitations such that secondary structures are suppressed.

C. Nanosphere of a doped semiconductor

As shown in Fig. 1, for a case with confined electron-phonon coupling, the electron-phonon scattering matrix $\rho(q)$ depends on the sphere radius and the electron doping concentration. The density of doped electrons can be controlled, but an actual typical density would be $10^{18}-10^{19}$ cm^{-3}. We study the absorption properties of the doped semiconductor sphere with the sphere radius R and the doped electron density parameter r_s. For GaAs, we collect the material parameters:[30] $\varepsilon_\infty=11.3$, $m^*=0.07$, $\omega_{LO}=36$ meV, and $\omega_{TO}=33$ meV. The most important energy scale is the plasmon energy ω_{pl}, which is given by $\omega_{pl}^2=4\pi n_0/\varepsilon_\infty m^*$ (n_0 is the electron density). $\gamma_{el}/\omega_{pl}=0.01$ and $\gamma_{ph}/\omega_{pl}=10^{-5}$ are taken.

Compared to the metallic case (given later), the plasmon energy ω_{pl} with the typical doping concentration is very small. Therefore, the energy difference of LO phonons and plasmons (actual relevant plasmon energy is $\omega_{pl}/\sqrt{\varepsilon_\infty}$ rather than ω_{pl}) is so small that they can be mutually coupled into new modes. Considering the dielectric response in the local limit of the *bulk* for the sake of simplicity, the pole structure of $1/\varepsilon(\omega)$ is determined by

$$\varepsilon_\infty \frac{\omega^2-\omega_{LO}^2}{\omega^2-\omega_{TO}^2}-\frac{\omega_{pl}^2}{\omega^2}=0,$$

from which we have two new modes $\omega_+(>\omega_{pl})$ and $\omega_-(<\omega_{TO})$. Analogues of these two modes and their branches of nonlocal peaks are observed in the nanoscopic spheres. If we assign the leading peaks of each branch to ω_+ and ω_- as indicated in Figs. 4 and 5, one can observe them in the unconfined case. However, in the confined case, we need introduce a certain cutoff radius R_c and can then have both ω_+ and ω_- only when $R>R_c$. R_c is determined by the condition that only a single zero, i.e., ω_+, is available in the zero structure of the dielectric response (for simplicity, in the nonlocal bulk),

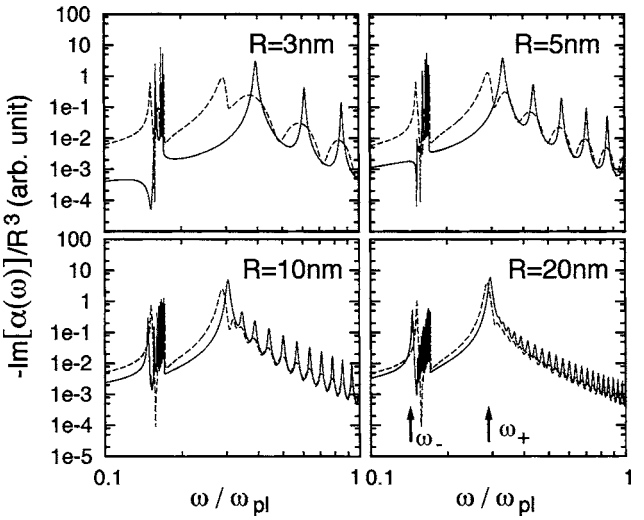

FIG. 4. Absorption of a doped GaAs sphere for $r_s=40$ ($n_0\sim 2.5\times10^{19}$ cm^{-3}, $\omega_{pl}=0.213$ eV) with respect to the sphere radius R. Here we have $\omega_{LO}/\omega_{pl}=0.17$ and $\omega_{TO}/\omega_{pl}=0.15$. The solid line is for the confined model and the dashed line for the unconfined model.

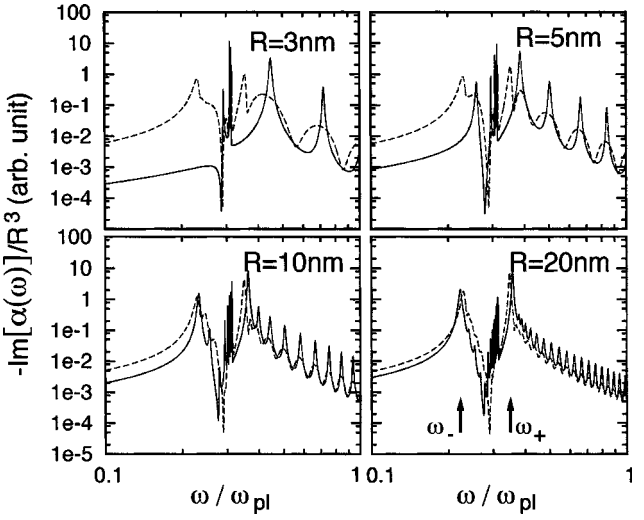

FIG. 5. Absorption of a doped GaAs sphere for $r_s=60$ ($n_0\sim 7.4\times10^{18}$ cm^{-3}, $\omega_{pl}=0.112$ eV) with respect to the sphere radius R. Here we have $\omega_{LO}/\omega_{pl}=0.32$ and $\omega_{TO}/\omega_{pl}=0.29$. The solid line is for the confined model and the dashed line for the unconfined model.

$$\varepsilon_\infty \frac{\omega^2-\omega_{\mathrm{LO}}^2}{\omega^2-\omega_{\mathrm{TO}}^2}-\frac{\omega_{\mathrm{pl}}^2}{\omega^2-\beta^2q^2}=0$$

for $q_{\min}(=\pi/R)$. It is further found that R_c is obtained by $q_{\min}=\omega_{\mathrm{TO}}/\beta$, from which we find $R_c=5.1$ nm for $r_s=40$ and $R_c=3.4$ nm for $r_s=60$. We actually observe that there is no resonance below ω_{TO} in cases of $R=3$ nm and $R=5$ nm in Fig. 4 and $R=3$ nm in Fig. 5. Nonlocal effects in the dielectric response give a series of phonon absorption peaks in region $\omega_{\mathrm{TO}}<\omega<\omega_{\mathrm{LO}}$ for q_n's where $\omega_{\mathrm{LO}}^2<\beta^2q_n^2$. Also, if there exist q_n's satisfying $\omega_{\mathrm{TO}}^2>\beta^2q_n^2$, phonon absorption peaks are also found for $\omega_-<\omega<\omega_{\mathrm{TO}}$. As R increases, q_n's can more probably satisfy $\omega_{\mathrm{TO}}^2>\beta^2q_n^2$ and absorption resonances for $\omega_-<\omega<\omega_{\mathrm{TO}}$ are obtained (see $R=10$ nm or $R=20$ nm in Fig. 5). However, actual modes in the present sphere with confined (or unconfined) phonons should be understood to occur at energies slightly shifted from the above poles because all the above discussions are provided based on the simple bulk model only with a quantization of wave vector. But a qualitative understanding is still possible.

In Figs. 4 and 5, the absorption depends on the electron density mainly through the plasmon energy ω_{pl}. For $r_s=60$ (Fig. 5) compared to $r_s=40$ (Fig. 4), ω_{pl} is closer to and more strongly coupled to ω_{LO}. For this reason, ω_+ ($\sim 0.33\omega_{\mathrm{pl}}$; $r_s=60$ and $R=20$ nm) in Fig. 5 is a bit shifted from the leading (surface) plasmon absorption in the system without phonons, $\omega_{\mathrm{pl}}/\sqrt{\varepsilon_\infty+2}=0.274\omega_{\mathrm{pl}}$. On the other hand, ω_+ in Fig. 4 is $0.28\omega_{\mathrm{pl}}$ (for $r_s=40$ and $R=20$ nm), so the shift is tiny. Thus the distance between ω_{LO} and ω_{pl} induces a repulsion between ω_- (redshift) and ω_+ (blueshift).

Although the report of phonon absorption in the doped semiconductor nanosphere, up to our knowledge, is not available, there is an interesting study of the phonon-assisted intraband transition in a cubic box modeled for a Si nanocrystal doped with one electron,[31] where intensities of the zero-phonon line and one-phonon line can be efficiently controlled by the geometry, i.e., size of the box. This work cannot be directly compared to our result but suggests how to go beyond our present approach.

D. Nanosphere of a metal

Previously, we have mentioned that metals can be treated in a similar way to doped semiconductors. Compared to a doped semiconductor, we note that ω_{LO} should correspond to the ion plasma frequency ω_{ip} and ω_{TO} should be zero in a metal. We also note that the density of conduction electrons is much higher than that in a doped semiconductor. We have typically $r_s\sim\mathcal{O}(1)$. Here, the optical absorption of an Al sphere is studied using the dielectric response $1/\varepsilon(q,\omega)$ explored in Sec. II D, which is, as a matter of fact, obtained from the free electron gas with the positive jellium background. For Al, we know $r_s=2.07$ and $\omega_{\mathrm{pl}}=15.8$ eV and we estimate the ion plasma frequency $\omega_{\mathrm{ip}}=122.8$ meV. Also, $\gamma_{\mathrm{el}}/\omega_{\mathrm{pl}}=0.01$ and $\gamma_{\mathrm{ph}}/\omega_{\mathrm{pl}}=10^{-5}$ are taken.

Unlike the case of a doped semiconductor, the ω_- mode does not exist in a metal. Instead, the phonon absorptions are located in $0<\omega<\omega_{\mathrm{ip}}$. In Fig. 6, we provide the optical absorption of an Al sphere in the (far-) infrared region. The

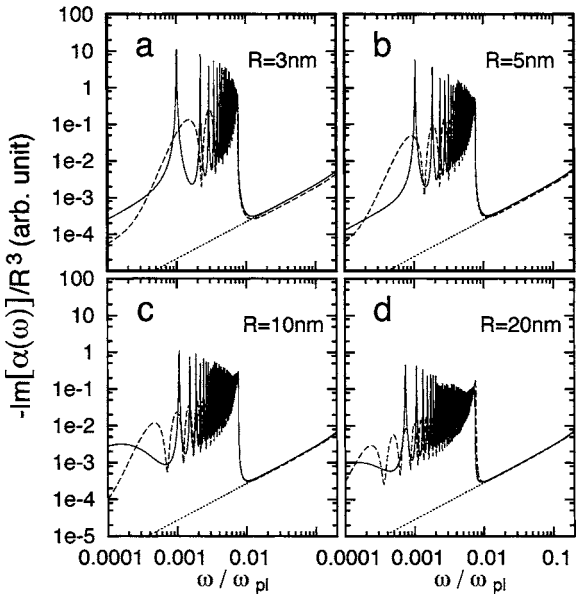

FIG. 6. Absorption of an Al sphere in the (far-) infrared region. The solid line is for the confined model, the dashed line for the unconfined model, and the dotted line for the confined model without phonon coupling. Note that the frequency ω of $\omega/\omega_{\mathrm{pl}}=0.0001$ corresponds to 1.58 meV or 12.7 cm^{-1}.

far-infrared absorption of various metal nanoparticles has been a controversial problem since an observation of anomalously enhanced far-infrared absorption in a dilute mixture of small metal particles.[32] A number of possible mechanisms intrinsic to isolated nanoparticles have been proposed. One of them is to include the electron-phonon coupling.[33,34] Also, the quantum size effects[5,6,35] or magnetic effects (eddy current loss)[36] were claimed to be responsible. A more realistic model to take into account the electron density profile has also been proposed.[37]

Now we show in Fig. 6 that the absorption in the given far-infrared energy range is enhanced by a few orders of magnitude by incorporating the electron-phonon coupling and is further reinforced by confinement along with the discrete nature. Such strong absorptions are found to be by short wavelength phonons. It is also found that, near the phonon absorption edge, an increase in the effective cross section by short wavelength phonons makes the absorption peaks have an accumulation point. By the way, it looks evident that long wavelength phonons hardly absorb the light in the given energy range, that is,

$$\frac{1}{\varepsilon_{\mathrm{sc-ph}}(q,\omega)}\propto\frac{\omega_{\mathrm{ip}}^2}{\omega_{\mathrm{pl}}^4}\frac{(\beta^2q^2)^2}{\omega^2-s^2q^2}$$

in the limit of $q\to 0$. s is the sound velocity. In spite of a formal similarity with the doped semiconductor, such appreciable differences referred to above are distinct in the spectra. Phonon absorptions are also found to depend on the sphere radius R. The absorption gets weaker on increasing the sphere size (see Fig. 6), which is consistent with the actual situation.[38] On increasing the radius, an anomalous absorption disappears and the classical (Mie) theory without phonons becomes valid, signifying that phonon contributions are less important for a larger sphere. This can be understood from Eq. (23) or (25); as $R\to\infty$, contributions from small q's

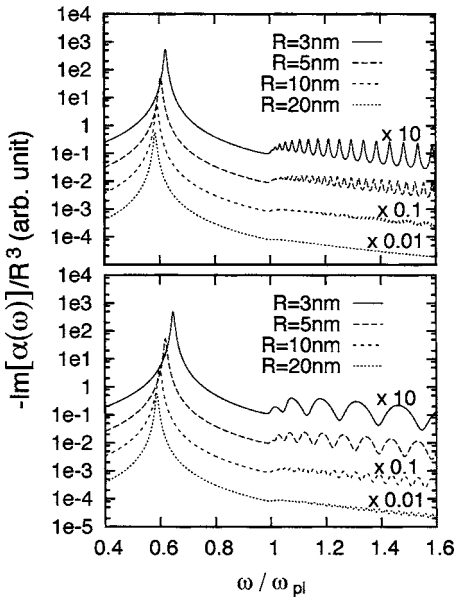

FIG. 7. Absorption of an Al sphere in the plasmon energy region. The upper panel gives the absorption for the confined model and the lower panel for the unconfined model.

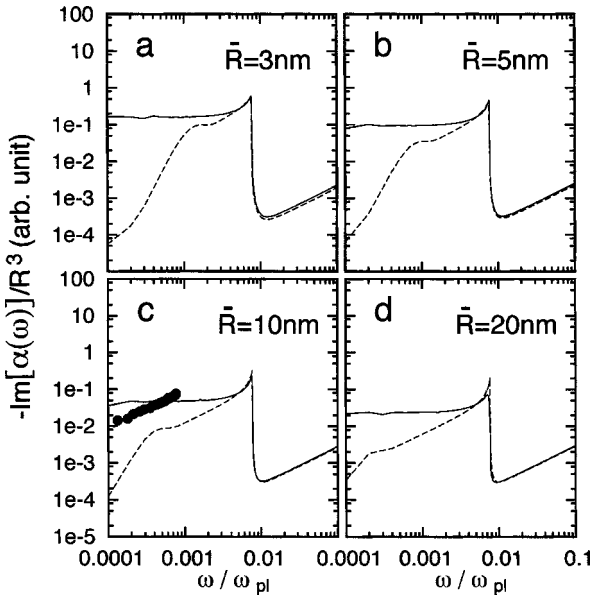

FIG. 8. Far-infrared absorption of an ensemble of isolated Al spheres with different R's. The solid line is for the confined model and the dashed line for the unconfined model. Note the differences in the spectra from two models, say, for energies of $\omega/\omega_{\mathrm{pl}} \lesssim 0.001$ (corresponding to $\omega \lesssim 15.8$ meV or $\omega \lesssim 127\ \mathrm{cm}^{-1}$). In (c), experimental results (black dots) for nonclustered Al composites ($\bar{R}=10.3$ nm) are given from Ref. 40. Experimental data are suitably modified in order to fit in our figure scale Ref. 41.

(actually $q \to 0$) become important by $[j_1(qR)]^2$ in the integral of E_1^{-1}, but for small q's ($q \to 0$), as argued above, the cross section for the absorption gets suppressed by $-\mathrm{Im}[1/\varepsilon_{\mathrm{sc-ph}}(q,\omega)] \propto q^3 \delta(\omega - sq)$. In our model, the far-infrared absorption converges to classical solution without phonons at about $R \approx 60$ nm.

Figure 7 shows the absorption of an Al sphere in the plasmon energy range for various R's. It is observed that the surface plasmon peak shifts to a higher energy on decreasing the sphere radius. In this energy range, the absorption occurs predominantly by creating a surface plasmon of $\sim \omega_{\mathrm{pl}}/\sqrt{3}$ ($\omega_{\mathrm{pl}}/\sqrt{3}$ is actually the value *in the local limit*). Above the plasmon energy ω_{pl}, one sees nonlocal secondary oscillations. These oscillations become less important as R increases, whereas the primary absorption at $\sim \omega_{\mathrm{pl}}/\sqrt{3}$ hardly changes in its strength.

E. Ensemble of metallic nanospheres with size distribution

To simulate the realistic situation, one may consider a medium composed of a random mixture of small particle constituents with respective dielectric responses $\varepsilon_i(q,\omega)$. Such a nanosphere ensemble can be considered by a random mixture of homogeneous spheres of different radii. Chylek and Srivastava[39] have proposed a γ-type size distribution function,

$$n(R) = aR^{\xi} e^{-bR},$$

where R is the sphere radius and a, b, and ξ are constants concerning the detailed distribution. From the distribution, we have the number density $\bar{n}$ given by

$$\bar{n} = \int_0^{\infty} dR\ n(R) = a \frac{\Gamma(\xi+1)}{b^{\xi+1}},$$

where $\Gamma(z)$ is the gamma function and the average radius of the spheres $\bar{R}$ is

$$\bar{R} = \frac{\xi}{b}.$$

Typically, for a given sample, one knows the average radius $\bar{R}$ and the filling factor f corresponding to $4\pi\bar{R}^3\bar{n}/3$. In Fig. 8, we give the far-infrared absorption of an ensemble of Al spheres with different $\bar{R}$'s. In $n(R)$, ξ is related to the variance of the distribution and the distribution goes like the delta function centered at $R=\bar{R}$ when $\xi \to \infty$. Here we put $\xi=10$. In particular, for a system of metallic spheres, the effect of size distribution can be essential. As seen in Fig. 6, the (far-) infrared absorption peaks are rapidly oscillating with the radius R, especially for the confined model. At $\omega/\omega_{\mathrm{pl}}=0.0001$ (corresponding to 1.58 meV or 12.7 cm^{-1}), for instance, there exists a set of closely spaced resonances (absorption peaks) which are swept through if the particle size changes only by ~ 0.25 nm. From the distribution function $n(R)$ with a fixed filling factor, it is found that, for $\bar{R}=3$ nm, most spheres belong to $2.0\ \mathrm{nm} < R < 4.3\ \mathrm{nm}$ [say, $n(2.0\ \mathrm{nm}) = n(4.3\ \mathrm{nm}) = 0.5n(\bar{R})$]; for $\bar{R}=5$ nm, $3.4\ \mathrm{nm} < R < 7.1$ nm; for $\bar{R}=10$ nm, $6.7\ \mathrm{nm} < R < 14.2$ nm; and for $\bar{R}=20$ nm, $13.4\ \mathrm{nm} < R < 28.4$ nm. In Fig. 8, we give the far-infrared absorption spectra averaged over the distribution $n(R)$ for the confined and the unconfined model with $\bar{R}=3, 5, 10, 20$ nm.

As a result of the average, a comparison of the absorption spectra becomes clearer. From Fig. 8, it is clear that the smaller spheres give the stronger absorption. Further, importantly, from a comparison between the spectra with and without confinement, we find that the confined phonons give much stronger far-infrared absorption in the region of very low energies. In addition, such strong absorption is quite robust down to $\omega/\omega_{\mathrm{pl}} \sim 0.0001$. Such dramatic differences are due to the fact that, in the confined model, sharp resonances can occur densely even in the far-infrared region with rapid sweepings by $\delta R \sim 0.25$ nm. In the unconfined model, on the contrary, there exists an energy scale for the absorption power to abruptly decrease, which depends on the radius. In Fig. 8(c), we have tried a direct comparison of our results with experiment. The experimental results in the figure[40] are the absorption for nonclustered Al particles ($\bar{R}=10.3$ nm) for $f=0.008$. The results agree with experimental observation in a qualitative view of the absorption strength. They are larger than the model of unconfined phonons by two orders of magnitude and than the model without phonons by four orders of magnitude near $\omega/\omega_{\mathrm{pl}} \sim 0.0001$. However, we do not claim that the confined electron-phonon interaction should be the only mechanism for the anomalous far-infrared absorption. The immediate reasons are that the actual experimental points have a large slope compared to almost constant theoretical results in the corresponding frequency region and the phonon absorption edge near ω_{ip} is too sharp compared to experiment,[1] which imply that remaining discrepancies should be explained by adding another mechanism, for instance, the clustering effects (interaction between nanospheres), classical magnetic dipole absorption, realistic dielectric surroundings, or the quantum mechanical particle-hole pair absorption, or others not included in this study. It is finally concluded that the electron-phonon coupling can give strong infrared absorption and a confinement of phonons can further enhance and stabilize the absorption in the far-infrared energy range for metallic nanospheres.

IV. SUMMARY AND CONCLUSIONS

We have studied the optical absorption of semiconducting and metallic nanospheres. In the nanoscopic geometry, relevant excitations in the system are quantized by quantum confinement. Considering only s-wave components of the excitations, they are quantized as $q_n R = n\pi$; $n=1,2,\ldots$ by a condition of $j_0(q_n R)=0$, where $j_0(x)$ is the spherical Bessel function of $l=0$. It is known that confined phonons interact with electrons in a different form of interaction compared to the bulk case. Taking into account such confinement, we have derived a coupling between electrons and phonons within spheres made of three different kinds of material: an intrinsic semiconductor, a doped semiconductor, and a metal. To investigate the optical absorption of the spheres, we took advantage of the semiclassical formalism of Fuchs and co-workers.[7] Their formalism is very useful in that it can be applied to any material with known dielectric response. However, we should mention a rather fundamental problem submerged in the formalism. In fact, the semiclassical theory of Fuchs and co-workers does not properly allow for the quantization of excitations, even if we have been motivated to do so due to its considerable merits. The cost of incorporating quantized excitations into the theory is the unclearness or arbitrariness of the boundary condition. It should be, therefore, understood that we have arbitrarily chosen one of applicable boundary conditions. More extended works to make clear the effect or importance of boundary conditions with respect to R may be required.

Let us summarize the work. First, for an intrinsic semiconductor sphere, the confinement effects are obvious. The electron-phonon scattering matrix $\rho(q)$ has a different form, which gives the enhanced infrared absorption and the slight redshift of absorption peak. Second, for a doped semiconductor (say a polaronic metal), the electron-phonon scattering matrix $\rho(q)$ depends on the doped electron density as well as the sphere radius. Two new branches (especially, leading absorption edges of them are called ω_- and ω_+, respectively) are developed in terms of a coupling between plasmon and LO phonon. For spheres of a small radius ($R<R_c$; see Figs. 4 and 5), however, we observe an explicit absence of the leading low energy absorption edge (ω_-) due to the finite smallness of q_{min} in the confined model. The continuous phonon absorption band is observed for $\omega_{\mathrm{TO}} \lesssim \omega \lesssim \omega_{\mathrm{LO}}$ by q_n's satisfying $q_n^2 \gtrsim \omega_{\mathrm{LO}}^2/\beta^2$ and also for $\omega_- \lesssim \omega \lesssim \omega_{\mathrm{TO}}$ for q_n's $q_n^2 \lesssim \omega_{\mathrm{TO}}^2/\beta^2$. Finally, we have studied the metallic sphere concentrating on the far-infrared energy region. Due to the electron screening, the ion plasma frequency (ω_{ip}) is softened into an acoustic phonon and the phonon absorption then occurs for $\omega \lesssim \omega_{\mathrm{ip}}$. The short wavelength phonons provide enhanced (far-) infrared absorption for both confined and unconfined models. It is important to find that confined phonons further reinforce the absorption. It now looks promising that the confined electron-phonon coupling possibly explains the anomalously enhanced absorption of various metal spheres. As R increases, the absorption coefficient decreases. Toward a realistic simulation, one may need to take into account the effect of size distribution. Assuming a given system as the random mixture of homogeneous spheres, we have examined effects of the size distribution of immersed metallic spheres. Above all, it is interesting and surprising that a confinement of phonons within a metallic sphere leads to not only the strongly enhanced absorption but also quite robust absorption even down to $\omega/\omega_{\mathrm{pl}} \sim 0.0001$, comparable to anomalously strong far-infrared absorption observed in experiment. However, it is also found that the detailed absorption behavior still differs from the known experimental data, which implies that incorporation of another mechanism as well as the confined electron-phonon interaction could be essential. To conclude, we affirm that the confined electron-phonon interaction should be enlisted among several possible mechanisms, even though it may not be enough by itself for a complete understanding of the anomalous experimental observations.

ACKNOWLEDGMENT

This work was supported by Special Coordination Funds for Promoting Science and Technology from the Ministry of Education, Culture, Sports, Science and Technology of the Japanese Government.

[1] C. F. Bohren and D. R. Huffman, *Absorption and Scattering of Light by Small Particles* (Wiley, New York, 1983); U. Kreibig and M. Vollmer, *Optical Properties of Metal Clusters* (Springer, Berlin, 1995).
[2] K. Cho, *Optical Responses of Nanostructures* (Springer, Berlin, 2003); C. Delerue and M. Lannoo, *Nanostructures* (Springer, Berlin, 2003).
[3] G. Mie, Ann. Phys. **25**, 377 (1908).
[4] L. P. Gorkov and G. M. Eliashberg, Zh. Eksp. Teor. Fiz. **48**, 1407 (1965); [Sov. Phys. JETP **21**, 940 (1965)].
[5] A. A. Lushinikov and A. J. Simonov, Z. Phys. **270**, 17 (1974); D. R. Penn and R. W. Rendell, Phys. Rev. B **26**, 3047 (1982).
[6] D. M. Wood and N. W. Ashcroft, Phys. Rev. B **25**, 6255 (1982).
[7] B. B. Dasgupta and R. Fuchs, Phys. Rev. B **24**, 554 (1981); F. Claro, *ibid.* **30**, 4989 (1984); R. Fuchs and F. Claro, *ibid.* **35**, 3722 (1987).
[8] K. L. Kelley, E. Coronado, L. L. Zhao, and G. C. Schatz, J. Phys. Chem. B **107**, 668 (2003).
[9] W. Eckardt, Phys. Rev. Lett. **52**, 1925 (1984); Phys. Rev. B **31**, 6360 (1985); **32**, 1961 (1985).
[10] R. Ruppin, Phys. Rev. B **45**, 11209 (1992).
[11] T. R. Jensen, G. C. Schatz, and R. P. Van Duyne, J. Phys. Chem. B **103**, 2394 (1999); T. R. Jensen, M. L. Duval, K. L. Kelley, A. A. Lazarides, and G. C. Schatz, *ibid.* **103**, 9846 (1999).
[12] C. Kittel, *Quantum Theory of Solids* (Wiley, New York, 1967).
[13] M. C. Klein, F. Hache, D. Ricard, and C. Flyutzanis, Phys. Rev. B **42**, 11123 (1990).
[14] S. Nomura and T. Kobayashi, Phys. Rev. B **45**, 1305 (1992).
[15] K. Huang and A. Rhys, Proc. R. Soc. London, Ser. A **204**, 406 (1950).
[16] C. Delerue, M. Lannoo, and G. Allan, Phys. Rev. B **68**, 115411 (2003).
[17] F. Giustino and A. Pasquarello, Phys. Rev. B **71**, 144104 (2005).
[18] G. D. Mahan, *Many-particle Physics* (Plenum, New York, 1986).
[19] See, for example, *Excitons*, edited by K. Cho (Springer, Berlin, 1979).
[20] The usual exciton Bohr radius is corresponding to a_0.
[21] S. Schmitt-Rink, D. A. B. Miller, and D. S. Chemla, Phys. Rev. B **35**, 8113 (1987).
[22] D. V. Melinkov and W. Beall Fowler, Phys. Rev. B **63**, 165301 (2001).
[23] M. Cini and P. Ascarelli, J. Phys. F: Met. Phys. **4**, 1998 (1974).
[24] In an actual case, a maximum cutoff value $l_{\max}$ of l can be considered. Counting the number of phonon modes, it should be $\propto N$ (N: the number of atoms in a sphere) and equal to $\sim N^{1/3}(l_{\max}+1)^2$. Thus, one finds $l_{\max}$ should be $\mathcal{O}(1)N^{1/3}$. For a typical nanosphere of $R=\mathcal{O}(10)$ nm, it includes $N=\mathcal{O}(10^3)$ atoms, leading to $l_{\max}$ to be $\mathcal{O}(10)$.
[25] In the metallic case, a difficulty of the presence of radial currents due to the dynamical nature of Maxwell equation occurs. To overcome the difficulty, Fuchs and co-workers Ref. 7 have suggested a new boundary condition. Finally, however, they found that the presence of radial current and a new boundary condition could hardly contribute to the absorption.
[26] It is not difficult to prove the relation up to a finite l using Riemann-Zeta functions $\zeta(s)$ with $s \leqslant 2l$, for example, one may prove up to $l=5$ using $\zeta(2)=\pi^2/6$, $\zeta(4)=\pi^4/90$, $\zeta(6)=\pi^6/945$, $\zeta(8)=\pi^8/9450$, and $\zeta(10)=\pi^{10}/93555$. But, in the same way, it is not immediately available to prove for a general value of l.
[27] R. Ruppin, Opt. Commun. **30**, 380 (1979).
[28] R. Zheng and M. Matsuura, Phys. Rev. B **56**, 2058 (1997).
[29] M. P. Chamberlain, C. Trallero-Giner, and M. Cardona, Phys. Rev. B **51**, 1680 (1995).
[30] A. Mooradian and G. B. Wright, Phys. Rev. Lett. **16**, 999 (1966).
[31] G. Allan and C. Delerue, Phys. Rev. B **66**, 233303 (2002).
[32] D. B. Tanner, A. J. Sievers, and B. A. Buhrman, Phys. Rev. B **11**, 1330 (1975).
[33] X. M. Hua and J. I. Gersten, Phys. Rev. B **31**, 855 (1985).
[34] P. Sheng, Phys. Rev. B **31**, 4906 (1985).
[35] R. Monreal, P. Andres, and F. Flores, J. Phys. C **18**, 4951 (1985).
[36] D. Stroud and F. P. Pan, Phys. Rev. B **17**, 1602 (1978).
[37] P. Apell, Phys. Scr. **29**, 146 (1984); A. V. Plyukhin, A. K. Sarychev, and A. M. Dykhne, Phys. Rev. B **59**, 1685 (1999).
[38] S. I. Lee, T. W. Noh, K. Cummings, and J. R. Gaines, Phys. Rev. Lett. **55**, 1626 (1985).
[39] P. Chylek and V. Srivastava, Phys. Rev. B **27**, 5098 (1983).
[40] Y. H. Kim and D. B. Tanner, Phys. Rev. B **39**, 3585 (1989).
[41] In Fig. 4 of Kim and Tanner Ref. 40, they have compared their data with classical calculation (i.e., theory with electric dipole only). We have manipulated the figure scale in order to make our zero-phonon result coincide with the classical calculation exhibited in their Fig. 4.